ABSTRACT

COUPLED OSCILLATORS: PROTEIN AND ACOUSTICS

by
Angelique N. McFarlane

This work encompassed three different vibrational energy transfer studies of coupled resonators (metal, topological, and microtubule comparison) inspired by the lattices of microtubules from regular and cancerous cells. *COMSOL Multiphysics 5.4* was utilized to design the experiment. The simulation starts with an acoustic pressure study to examine the vibrational modes present in coupled cylinders, representing α-, β-tubulin heterodimers. The Metal Study consisted of 3 models (monomer, dimer, and trimer) to choose the correct height (40 mm) and mode (Mode 1) for study. The Topological Study was run to predict and understand how the lattice structure changes over a parametric sweep (Qian et al. [7]). This study includes a Su-Schrieffer-Heeger Model for prediction, then a Model inspired by the microtubule protofilament. Finally, a new proposed method is given to simulate a microtubule. Study 3 has 2 models, both with a two-dimensional lattice, but the second with two distinct domains to emulate the 80 % - 20 % healthy/cancerous regions within a cancerous microtubule. The spectrums from each model is inspired by the microtubule-associated proteins (MAPs) bound to the tubulin dimers, in Region 1, then unbinding in Region 2. The Cancerous Model shows less energy held within the lattice as compared to the Microtubule Model. Future work could involve changing the coupling strengths and distances to conform to schematics from Martínez et al. [5] and Deniz et al. [4].

COUPLED OSCILLATORS: PROTEIN AND ACOUSTICS

by
Angelique N. McFarlane

A Thesis
Submitted to the Faculty of
New Jersey Institute of Technology
in Partial Fulfillment of the Requirements for the Degree of
Master of Science in Materials Science and Engineering

Department of Physics

August 2022

Blank Page

BIOGRAPHICAL SKETCH

Author: Angelique N. McFarlane

Degree: Master of Science

Date: August 2022

Date of Birth:

Place of Birth:

Undergraduate and Graduate Education:

- Master of Science in Materials Science and Engineering,
  New Jersey Institute of Technology, Newark, NJ, 2022

- Bachelor of Science in Physics and Chemistry,
  Seton Hall University, South Orange, NJ, 2019

Major: Materials Science and Engineering

This work is dedicated to my mother, Shirley Chambers-McFarlane.

Thank you for being my first teacher and my best friend. You have been the only one by my side through the challenges of teaching, school, and the struggles with my faith. You were and still are my model for success and womanhood. I know no matter what, I have you. I hope to be half the woman and mother you are one day.

This year has been tough, but we got through it together. Let's celebrate in Disney World!

Love you always, Angie.

ACKNOWLEDGMENT

TABLE OF CONTENTS

LIST OF TABLES

LIST OF FIGURES

Figure   **Page**

CHAPTER 1

INTRODUCTION

This chapter provides a brief explanation of the major topics discussed within this work and ends with the purpose of the study.

1.1 Microtubule

1.1.1 Basic Functions

Microtubules are one of the three cytoskeletal elements within eukaryotic cells. They are key players within cell movement, cell division, and cell transport. Microtubules provide structure to cilia and flagella, form mitotic spindles, and aid organelle movement within the cytoplasm respectively.

Experimentally Grown Guanosine-5'-[(α,β)-methyleno]triphosphate (GMPCPP) Microtubules visualized using Fluorescence Microscopy. The picture shows multiple double (coupled) microtubule strands in vitro floating in a Tubulin PEM buffer solution.
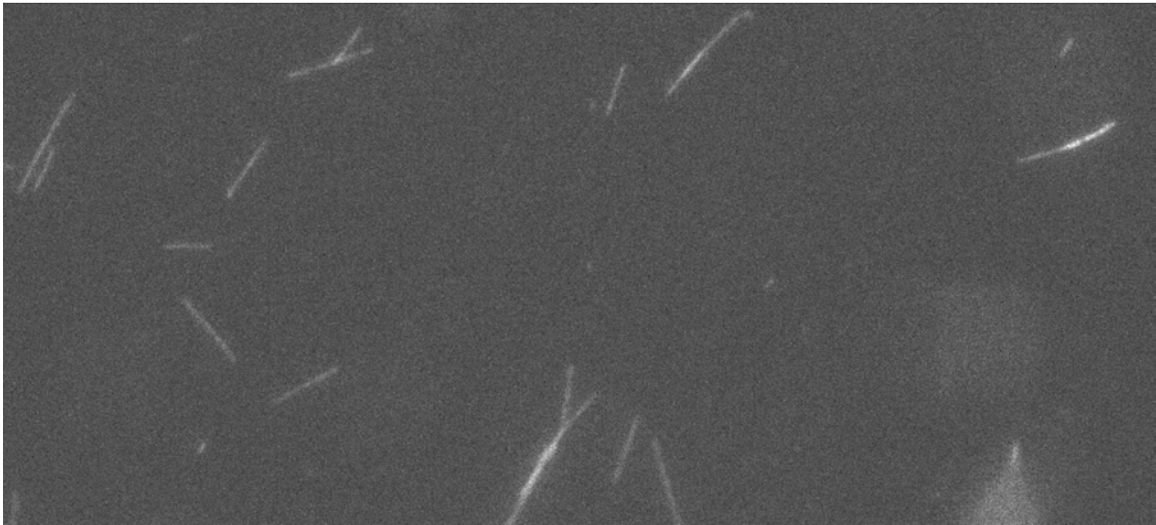
Figure 1.1 Experimentally grown GMPCPP microtubules.

1.1.2 Lattice Structure

The uniqueness of microtubule structure allows for its various uses. Microtubules are hollow, rigid, and cylindrical polymers. They can grow to lengths of 50 µm making it the largest cytoskeletal element. The inner diameter is between 11 – 15 nm and the outer diameter is between 23 – 27 nm. The microtubule polymer is composed of two globular proteins, α- and β- tubulin. These proteins form heterodimers, two

The lattice structure of a microtubule. a) The microtubule heterodimer composed of α-,β-tubulins. These proteins bind together to form the lattice. b) The microtubule protofilament which has an α-tubulin end (minus -) and a β-tubulin end (plus +). Each protofilament has multiple heterodimers covalently bound together. Protofilaments align themselves laterally to form the linear structure. c) The aerial view of the microtubule lattice. Once the protofilaments align, the microtubule gains a cylindrical shape with the inside being hollow. The picture shows a diameter of 14 nm. d) The microtubule's side view. The protofilaments will align in the same direction (direction of arrow) and give the microtubule an outer diameter of ≈ 25 nm.

d) Microtubule Side View

25 nm

c) Microtubule Aerial View

a) Microtubule Heterodimer

β-tubulin

α-tubulin

14 nm

b) Microtubule Protofilament
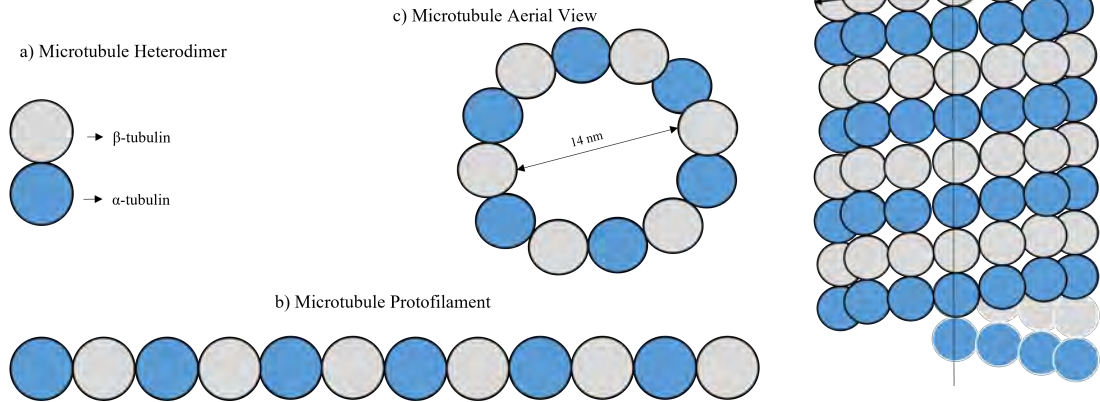
Figure 1.2 Microtubule structure.

distinct monomers non-covalently bound. The α- and β- tubulin dimer can then bind together and form protofilaments. Protofilaments are a linear collection of α- and β- tubulin heterodimers. The protofilament can then align itself laterally and bind with other protofilaments to form the microtubule. Microtubules typically have 13 protofilaments within the lattice structure.

1.2 Introduction to Topology

Topology is a branch of mathematics concerned with the conserved geometry of objects under deformations. Allowed deformations include stretching, twisting, crumpling, and bending. If the object in question preserves its geometry under these

conditions, it has topological invariance. An example of topological invariance arises in the continuous deformation of a coffee mug to a donut (torus). Since both objects only have one hole (the dip in the mug does not count as a hole), a coffee mug can easily be transformed to a donut and vice versa. Both objects maintain their geometry and properties.

Visual explanation of how homeomorphism works within topology. A coffee cup can morph into a donut because both structures only have one hole. If no tearing or gluing occurs, then deformations are allowed to transform one into another.
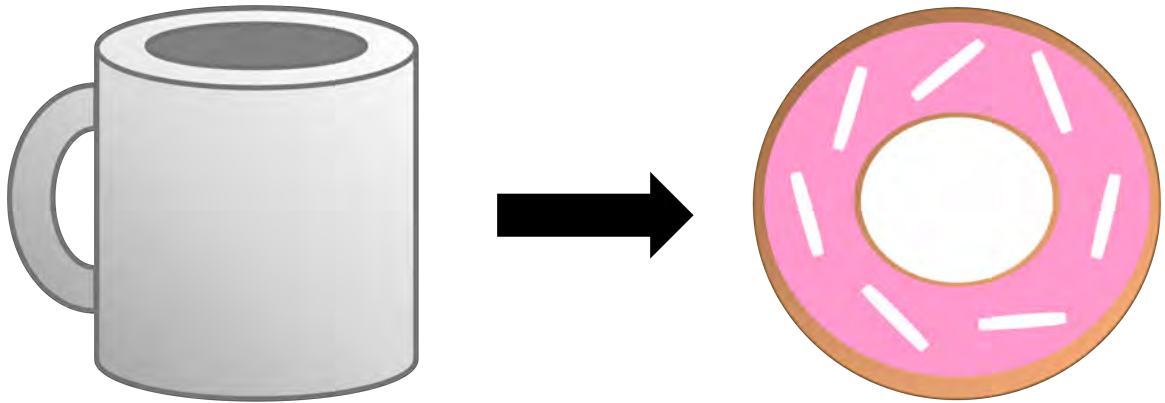
Figure 1.3 Homeomorphism in topology.

1.2.1   Topological Insulators

A topological insulator is a material which behaves as an insulator in its interior, but its edges are conducting. A depiction of an insulator is provided in Fig. 1.4. An electrical topological insulator occurs when a magnetic field passes through a thin metal sheet. The inner electrons align with the magnetic field and are trapped within a closed orbit. Because the electrons are trapped, they are not conducting. In contrast, the electrons along the edge of the sheet are open. These electrons jump from orbit to orbit (in one direction), creating conduction along the edge. The material's conduction is not affected by deformations, making topological invariant. Typically, deformations would inhibit conduction, but the uniqueness of the material allows for conduction to occur.

A topological insulator conducting electrically along the edge of the material. The magnetic field passes through the metal sheet and traps the inner electrons in orbit. The electrons along the edge begin travelling across the edge, making the edge conducting.

Magnetic Field

Metal Sheet

Conducting Electrons

Electrons trapped within orbit
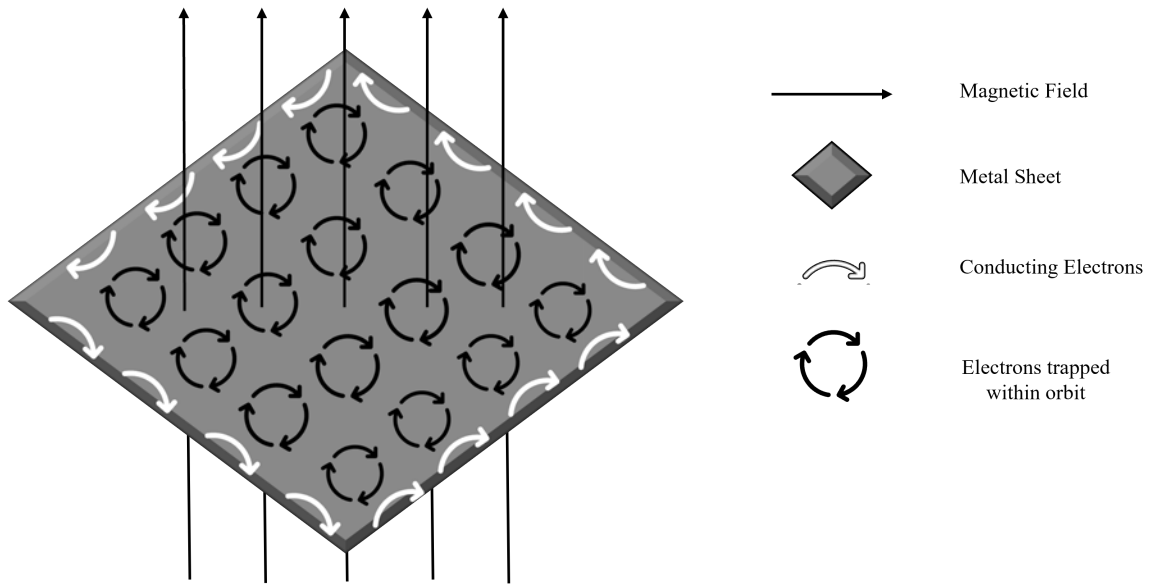
Figure 1.4 Topological insulator.

1.3 Acoustics, Phonons, and Coupled Oscillators in Proteins

Acoustics is the branch of physics that focuses on sound, a pressure wave created by the object's vibration. It focuses on the mechanical waves that propagate through materials and the resulting vibrations. In solid-state and condensed matter physics, the phonon is the highlight of study. Phonons are considered quantized sound waves within condensed phases of matter. They have similar properties to photons, but phonons of different wavelengths can interact. These interactions are studied within condensed matter physics.

An oscillator is a system that returns to its equilibrium position when displaced. If two oscillators are coupled together, energy can be transferred from one oscillator to another. The vibration from the initial system will interrupt the second system. This is the process believed to occur within proteins. Fig. 1.5 provides a visual explanation of how the mechanical waves of the second system is a result of the first.

Depiction of two coupled pendulums oscillating. The red oscillator behaves as the system's resonator. The oscillation of the red will dictate the oscillations of the green. Portions of the waveguides have deconstructive interference (zero) and others constructive (1,-1).
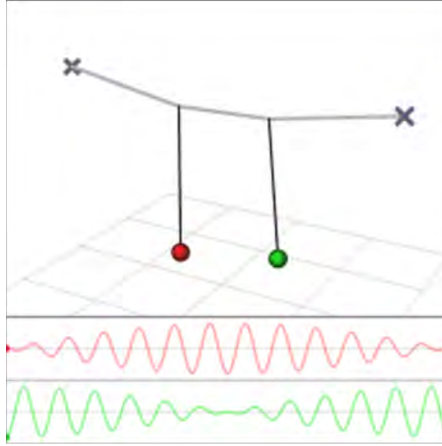
Taken from:
https://phys.libretexts.org/Bookshelves/University_Physics/Book:_Mechanics_and_Relativity_(Idema)/08:_Oscillations/8.0
4:_Coupled_Oscillators

Figure 1.5 Depiction of two coupled oscillators.

1.4 Resonators in Proteins and Acoustics

A resonator is an external system that disrupts the internal system. The resonator's driving force will interrupt the internal and force vibrations into the system. Within proteins, the resonator is believed to be the end molecules. Fig. 1.6 shows polyacetylene within the Su-Schrieffer-Heeger (SSH) Model, which describes how spinless fermions hop across a one-dimensional lattice. One portion of the molecule is high pressure and the other low pressure. Like how coupled oscillators transfer energy from one system to another, the molecules in polyacetylene will transfer vibrations from the high end to the low end. Microtubules are shown to have the same ability (Prodan and Prodan [6]).

Polyacetylene Molecule in Su-Schrieffer-Heeger (SSH) Model. The SSH Model is a tight-binding model that describes a single spin-less on a two-site unit cell 1D lattice. It is used in low-dimensional condensed matter systems such as the polyacetylene molecule.
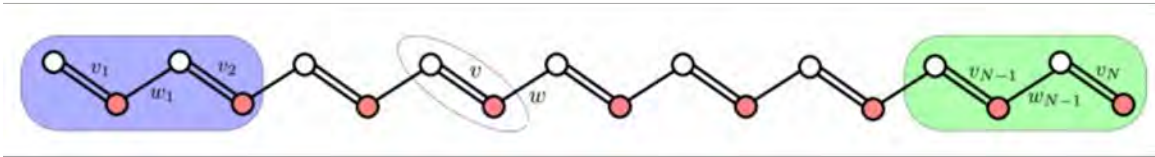
Figure 1.6 Polyacetylene molecule in Su-Schrieffer-Heeger (SSH) model.

1.5 Goal of Study

Microtubules are believed to be one-dimensional phononic topological insulators (Apigo et al. [1], Prodan and Prodan [6], Qian et al. [7]). Microtubules are shown to permit vibrations to pass through its lattice. This vibrational transfer has shown to be topologically invariant. This project aims to propose a new method to analyze topological edge modes in microtubules taken from noncancerous and cancerous cells.

Microtubules from cancerous cells do not hold as much energy within its lattice due to its different lattice structure. This means vibrational transfer will propagate through the system differently. The topological edge modes in microtubules from noncancerous and cancerous cells were studied using a simulated cylinder structure in *COMSOL Multiphysics 5.4*. The acoustic simulation will solve the cylinder's eigenfrequencies. The best height will be found by performing a simulated monomer, dimer, and trimer study. Then, the cylinder will be dimerized within the SSH Model to examine the first mode of vibration. Lastly, a protofilament will be generated to analyze how energy is transferred in the microtubule. This will be paired with a pressure acoustic simulation of microtubules from noncancerous and cancerous cells.

CHAPTER 2

PRESSURE ACOUSTICS PROTOCOLS

This chapter outlines the protocols used for the acoustic and protein study.

Steps for building the Models in *COMSOL Multiphysics 5.4*. The radius (*r*), length (*l*), position (*x, y, z*), and axis type (*z-axis for cylinders; x-axis for couplings*) were set within "Component 1" in the "Geometry" tab
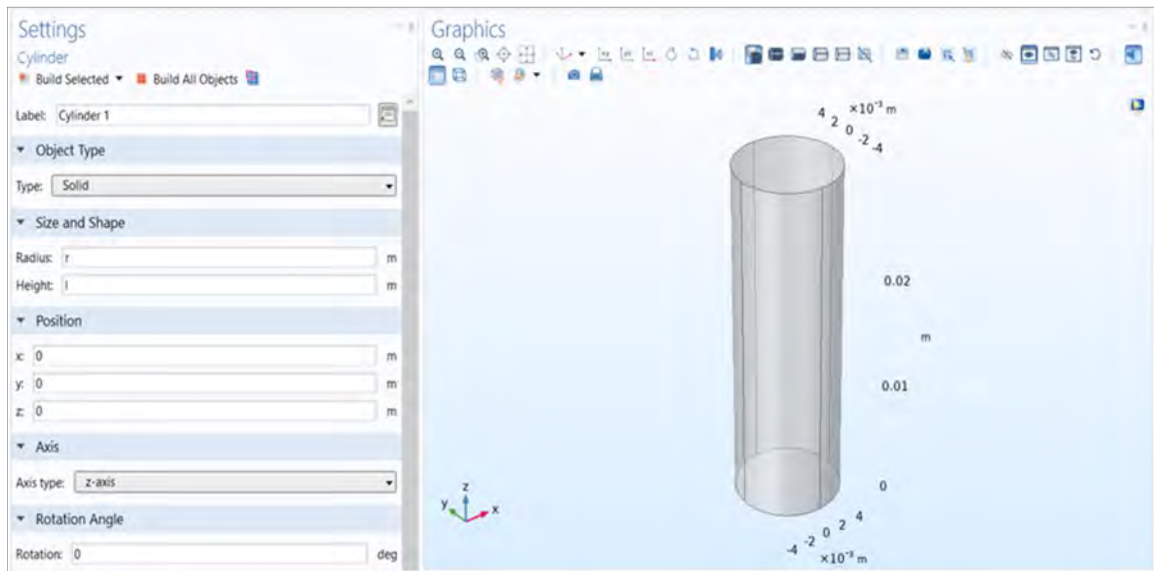
Figure 2.1 Building the models in *COMSOL Multiphysics 5.4*.

2.1 Simulation Environment

The program *COMSOL Multiphysics 5.4* was used to perform the acoustic study. To begin the simulation, the correct environment had to be created. To do this, the "Model Wizard" option was chosen, the space dimension was set to "3D", and the physics was set to "Acoustics", "Pressure Acoustics" and "Frequency Domain." Then, an "Eigenfrequency" study was added. After the correct environment was made, the cylinder's variables were input. Radius was set to r, length to l, the distance between the cylinders to d, and the radius of coupling to $r2$. The monomer study did not include d or $r2$ and tested three different lengths (30 mm, 40 mm, and 50 mm). The

7

Table 2.1 Metal Study Parameters

Metal Study Parameters		
Name	Value	Description
r	5 mm	radius of cylinder
l	30 mm, 40 mm, or 50 mm	length of cylinder
d	15 mm	distance between cylinders
r2	1 mm	radius of coupling

dimer and trimer studies had $r = 5$ mm, l $= 40$ mm, $d = 15$ mm, and $r2 = 1$ mm. The remaining variables were $r = 5$ mm, $l = 40$ mm, $d = 15$ mm. Then, the variables were used to build the cylinders and couplings for each study. The build parameters for the Metal Study are are outlined in Table 2.1.

The exact study desired had to be added to run the simulation. First, air was added to the system through the "Add Materials" tab. Next, a mesh is needed to divide the geometry. This is added by selecting "Physics-controlled mesh" under "Mesh 1" in the Sequence Type tab. For each study, the resulting eigenfrequencies needs to have enough separation from the next frequency for there to be a topological gap in the SSH model spectrum. To ensure this, "Eigenfrequency" was selected under "Study 1" and the "Desired number of eigenfrequencies" set to 6 for the metal study (monomer, dimer, and trimer) and the number of cylinders present for the remaining (SSH, Protofilament, Microtubule, Cancerous) studies. In addition, 4000 Hz was chosen for the "Search for eigenfrequencies around" option.

2.2   Parametric Sweep

Finally, "Parametric Sweep" was chosen under "Study 1", and, in the parameter value list, the following was selected: 11 mm for start, 1 mm for step, and 20 mm for

stop. The former values were used for the metal study. For the SSH and Protofilament parametric sweep studies, -4 mm was used for start, 0.5 mm for step, and 4 mm for stop. The parametric sweep was evaluated for the parameter m = -4 mm. This was to allow the average distance between cylinders to change at the same time. For the Microtubule and Cancerous Models, the parametric sweep was evaluated over lattice coupling distance. The start was set to 11 mm, step was set to 0.5 mm, and the stop was set to 20 mm. Once everything was completed, the eigenfrequency was computed.

Table 2.2 Topological Study Parameters

Topological Study Parameters		
Name	Value	Description
r	5 mm	radius of cylinder
l	40 mm	length of cylinder
davg	15 mm	average distance between cylinders
r2	1 mm	radius of coupling
d1	d+m	distance between weaker coupling
d2	d-m	distance between stronger coupling
m	-4 mm	parametric sweep value
k	0	wave vector

2.3   Additional Parameters

The SSH and protofilament models required the cylinders to be dimerized (paired together like the α-, β-tubulin heterodimer) and then coupled to multiple dimers. To do this, new parameters $davg$ =15 mm (average distance between cylinders), $d1$ = d+m (distance between the weaker coupling), and $d2$ = d-m (distance between the stronger coupling) were introduced. The average distance

(davg) had to agree with the condition $davg > 2r+m$. The SSH Model had 8 cylinders (2 single cylinders and 3 pairs) while the Protofilament Model had 20 cylinders (2 single cylinders and 9 pairs).

The Microtubule and Cancerous Models were dimerized, then coupled in a lattice. There were 5 rows of 20 cylinders (2 single cylinders and 9 pairs). Both introduced $d3 = 15$ mm for the Microtubule Model and 19 mm for the Cancerous Model. For the Cancerous Model, parameters $d4 = 14$ mm and $d5 = 20$ mm were added. This was for the cancerous region of the lattice.

The wave vector had to be defined for each of these models. The parameter k was set to "0" within the "Global Definitions," "Parameters 1" tab. Then, under "Component 1 in the "Pressure Acoustics, Frequency Domain" tab, the type of periodicity was changed to "Floquet periodicity" in the "Periodic Condition 1" window. The following values were set for the SSH and Protofilament models: $x = $ kx, $y = 0$, $z = 0$. Lastly, the following values were set for the Microtubule and Cancerous models: $x = $ kx, $y = $ ky, $z = 0$.

The parametric sweep values for each study. a) The Metal Study (Monomer, Dimer, and Trimer) parameters evaluated over the distance between cylinders, *d*. b) The Topological Study (SSH & Protofilament) parameters (evaluated over m, -4 to 4 iterating over 0.5. c) The Microtubule & Cancerous parameters (evaluated over the lattice coupling distance, *d3*).

a) Parametric Sweep Values for the Metal Study	b) Parametric Sweep Values for the Topological Study	c) Parametric Sweep Values for Microtubule & Cancerous Models
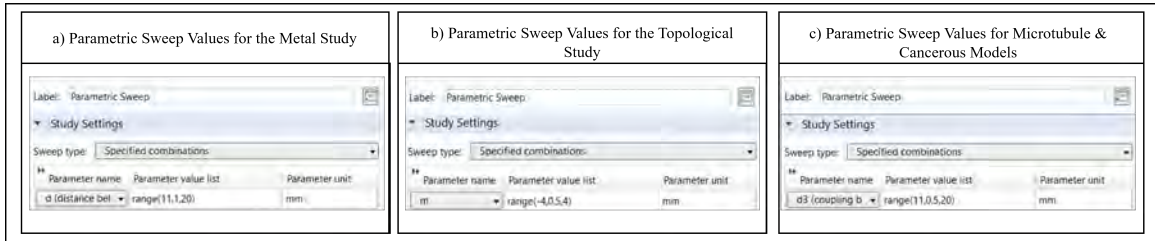
Figure 2.2 Parametric sweep values for metal, topological, and microtubule studies.

Table 2.3 Microtubule Study Parameters

Microtubule Study Parameters		

Microtubule Model Parameters

Name	Value	Description
r	5 mm	radius of cylinder
l	40 mm	length of cylinder
davg	15 mm	average distance between cylinders
r2	1 mm	radius of coupling
d1	d+m	distance between weaker coupling
d2	d-m	distance between stronger coupling
m	-4 mm	parametric sweep value
k	0	wave vector
d3	15 mm	lattice coupling

Cancerous Model Parameters

Name	Value	Description
r	5 mm	radius of cylinder
l	40 mm	length of cylinder
davg	15 mm	average distance between cylinders
r2	1 mm	radius of coupling
d1	d+m	distance between weaker coupling
d2	d-m	distance between stronger coupling
m	-4 mm	parametric sweep value
k	0	wave vector
d3	19 mm	lattice coupling
d4	14 mm	distance between weaker cancerous coupling
d5	20 mm	distance between stronger cancerous coupling

METAL & TOPOLOGICAL STUDY

In the metal study, no topological gaps are observed. However, the results from this investigation will be used to design the topological investigation. Three different lengths from 30 mm - 50 mm were used, and the best length was placed in the SSH Model to predict the topology of the system. Then, the SSH Model was extended to 20 cylinders to create the Protofilament Model.

3.1   Metal Study

Modes for 30 mm Monomer Model. a) Zero mode; b) first mode; c) second mode; d) third mode; e) fourth mode; f) fifth mode; g) sixth mode; h) seventh mode; and i) eighth mode. The modes begin repeating at the fourth mode (e), indicating there is not enough separation between the frequencies for a topological study even though the frequency separation was $\approx$ 5720 Hz.
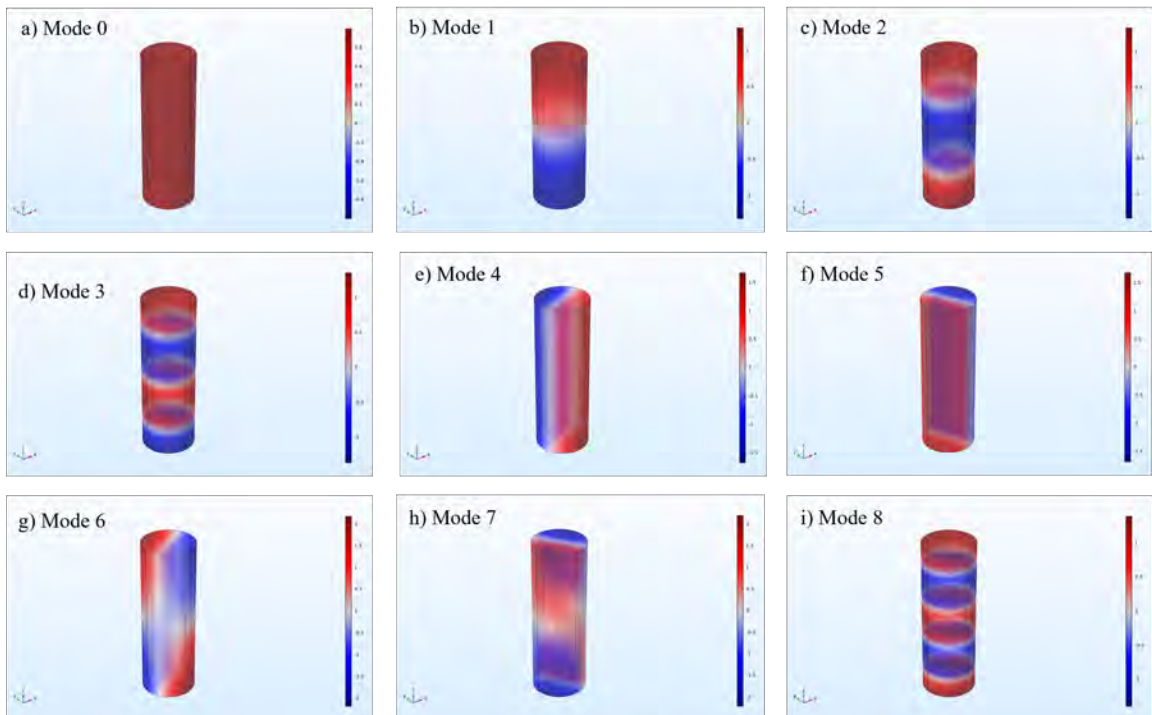
Figure 3.1 Modes for 30 mm monomer model.

Table 3.1 Frequencies for Monomer Model

Frequencies for Monomer Model					
30 mm Monomer		40 mm Monomer		50 mm Monomer	
Mode	Eigenfrequency (Hz)	Mode	Eigenfrequency (Hz)	Mode	Eigenfrequency (Hz)
1	5720	1	4290	1	3432
2	11440	2	8580.1	2	6864
3	17163	3	12871	3	10296
4	20120	4	17164	4	13730
5	20121	5	20122	5	17165
6	20918	6	20122	6	20123
7	20919	7	20574	7	20125
8	22892	8	20575	–	–

The Monomer Model tested a single cylinder of lengths 30 mm, 40 mm, and 50 mm. The resulting eigenfrequencies are outlined in Table 3.1. The first 3 modes for the 30 mm model had a separation of $\approx 5720Hz$. However, Modes 4 – 8 and little separation between each other and had repeating frequencies. The 40 mm model had a separation of $\approx 4290Hz$ between Modes 1 – 4. Modes 5 – 8 began repeating. The 50 mm model had seven modes instead of eight. Modes 1 – 5 had a separation of $\approx 3432Hz$ with Modes 6, 7 repeating. The separation corresponded with the value of the Mode 1. The eigenfrequency had to have enough separation between each mode to continue the investigation. Also, the modes had to have minimal repetition. This made the 40 mm model the best for analysis.

3.2 Dimer & Trimer Models

The Dimer and Trimer Models were designed to analyze how each of the modes split. For example, in the Dimer Model, the first three modes from the monomer

Modes for 40 mm Monomer Model. a) Zero mode; b) first mode; c) second mode; d) third mode; e) fourth mode; f) fifth mode; g) sixth mode; h) seventh mode; and i) eighth mode. The modes begin repeating at the fifth mode (f), indicating there is enough separation between the frequencies for a topological study. The frequency separation was ≈ 4290 Hz, which is enough for a topological gap to appear.
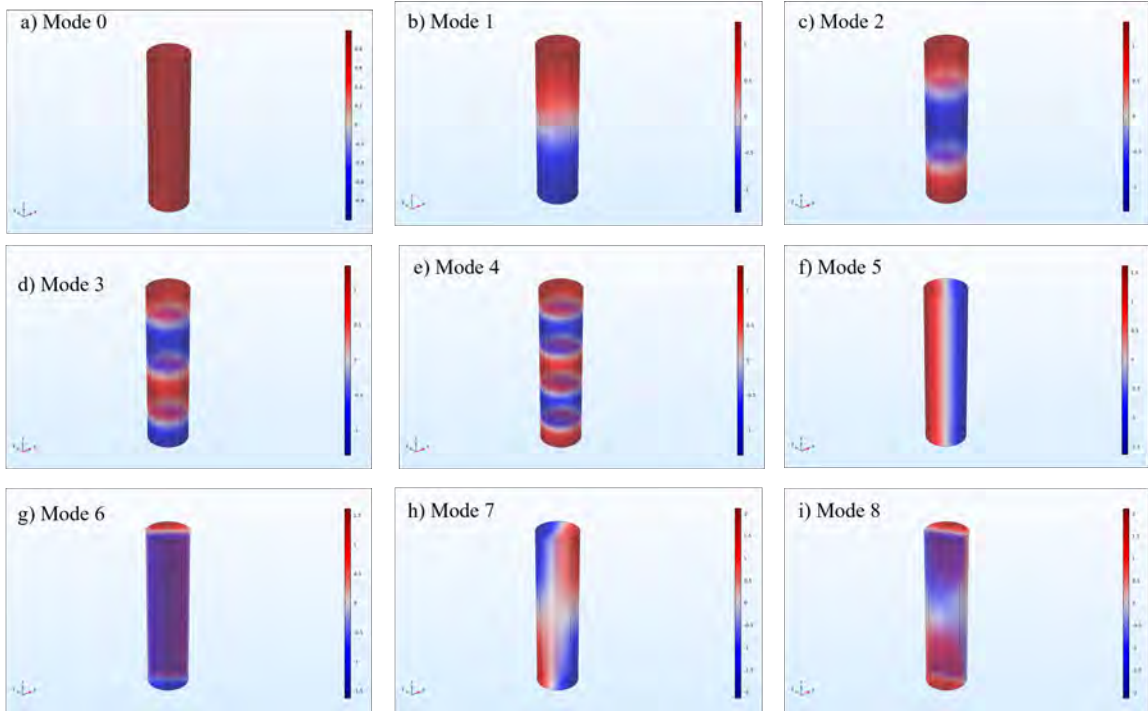
Figure 3.2 Modes for 40 mm monomer model.

study (4290 Hz, 8580.1 Hz, and 12871 Hz) were separated into two eigenfrequencies (Mode 1 – 4219.2 Hz, 4617.4 Hz; Mode 2 – 8505.4 Hz, 8654.8 Hz; Mode 3 – 12820 Hz, 12902 Hz) which corresponds to the number of cylinders present. The splitting occurs because two separate oscillating systems were coupled.

Mode 1 was chosen to further analysis and put into the Trimer Model. Here Mode 1 was split into three resulting in eigenfrequencies of 4195.3 Hz, 4409.3 Hz, and 4772.3 Hz. Again, there was enough separation within the eigenfrequencies to further investigation.

Modes for 50 mm Monomer Model. a) Zero mode; b) first mode; c) second mode; d) third mode; e) fourth mode; f) fifth mode; g) sixth mode; and h) seventh mode. The modes begin repeating at the sixth mode (g), indicating there is enough separation between the frequencies for a topological study. However, the frequency separation was ≈ 3432 Hz, which is too small for a topological gap to appear.
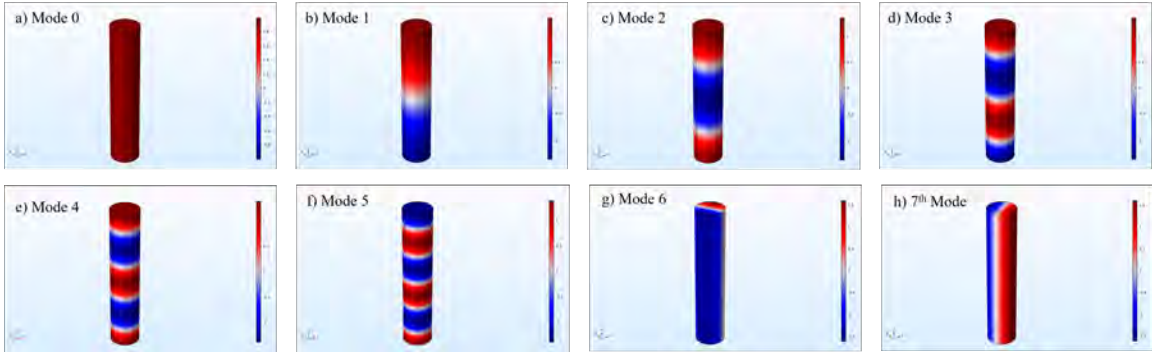
Figure 3.3 Modes for 50 mm Monomer Model.

Table 3.2 Frequencies for 40 mm Dimer & Trimer Models

Frequencies for 40 mm Dimer & Trimer Models			
Dimer Model		Trimer Model	
Mode	Eigenfrequency (Hz)	Mode	Eigenfrequency (Hz)
1.1	4219.2	1.1	4195.3
1.2	4617.4	1.2	4409.3
2.1	8505.4	1.3	4772.3
2.2	8654.8	–	–
3.1	12820	–	–
3.2	12902	–	–

3.3 Su-Schrieffer-Heeger & Protofilament Models

The SSH and Protofilament Models had to have infinite and periodic boundary conditions. This was to emulate a structure that could repeat itself without the need for designing a large structure, requiring a higher computational cost. To create these conditions, the end cylinders were left unpaired (single cylinder). Then, the end

Figure 3.4 Modes for 40 mm dimer model.

coupling length was halved (*d2/2*). This allowed infinite, periodic conditions. The same process was used for the Microtubule and Cancerous Models.

The SSH Model composed of 2 single, end cylinders and 3 pairs of dimerized cylinders all coupled together. The eigenfrequencies of Mode 1 split into 8 and occurred at 4272.8 Hz, 4322.9 Hz, 4323.1 Hz, 4390.4 Hz, 4720.6 Hz, 4789.8 Hz, 4801.4 Hz, and 4853.4 Hz. Modes 1.2 (4322.9 Hz), 1.3 (4323.1 Hz), 1.6 (4789.8 Hz), and 1.7 (4801.4 Hz) in the acoustic pressure diagram show portions of the model that do not oscillate easily. The calculated eigenfrequencies are outlined in Table 3.3.

The spectrum indicates Mode 1 has topological properties. The portion of the curve that crosses (occurring at 0 mm) indicates the system behaves as a metal. The gaps to the left and right indicate topological properties. The left portion has trivial topology and the right non-trivial topology.

Within the trivial portion, no vibrations can perturb the phonons enough to cause oscillations. Therefore, the bulk is insulating. Within the non-trivial portion, there is a strong enough phonon interactions for the waves to interfere. The result is

Modes for 40 mm Trimer Model. The first mode was split into three modes (the number of cylinders present). Pictures a), b), and c) show how the acoustic pressure is split (4195.3 Hz, 4409.3 Hz, and 4772.3 Hz respectively). Mode 1 was used to further the topological investigation.
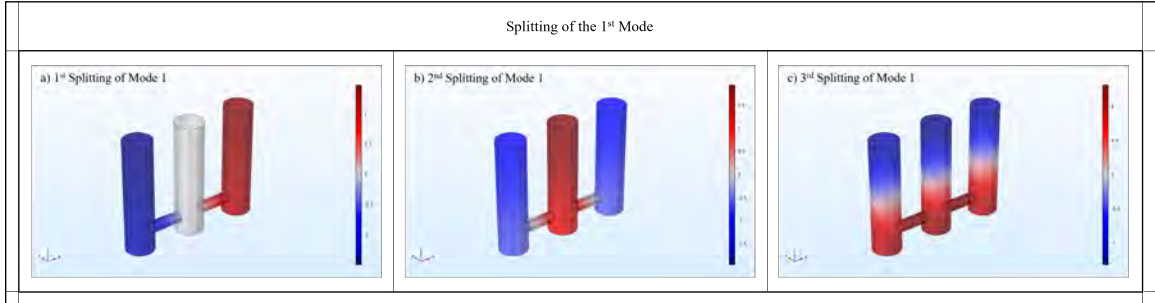
Figure 3.5 Modes for 40 mm trimer.

Modes for Su-Schrieffer-Heeger (SSH) Model. Here, the cylinders are dimerized (paired) then coupled to other dimers, like the microtubule heterodimers. Mode 1 was used to predict the behavior of the Protofilament Model and was split into eight modes. a) Mode 1.1 (4242.8 Hz), b) Mode 1.2 (4322.9 Hz), c) Mode 1.3 (4323.1 Hz), d) Mode 1.4 (4390.4 Hz), e) Mode 1.5 (4720.6 Hz), f) Mode 1.6 (4789.8 Hz), g) Mode 1.7 (4801.4), and h) Mode 1.8 (4853.4 Hz). The clear colored cylinders are portions of the acoustic waveguide which are zero pressure (not oscillating or not oscillating easily.
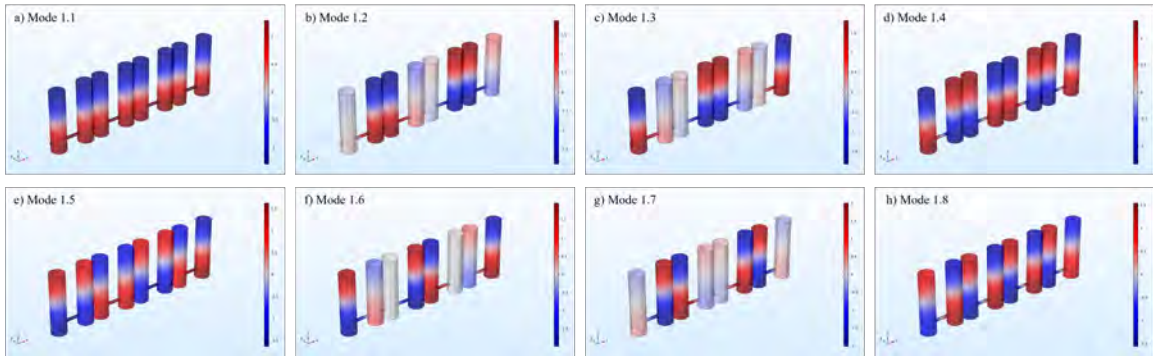
Figure 3.6 Modes for Su-Schrieffer-Heeger (SSH) model.

a structure that is topologically different than the trivial. In fact, the band structure can begin to twist. It can be assumed the system has chiral edge modes within the non-trivial topology portion (Cheng et al. [3]).

The Protofilament Model displays the same characteristics as the SSH. Here, there are 2 single end cylinders and 9 pairs of dimerized cylinders, all coupled together. The spectrum is similar, but with a larger bulk due to the increased number of cylinders.

Like the SSH Model, there are portions of the acoustic pressure diagram that do not oscillate easily at Modes 1.3 (4281.7 Hz), 1.4 (4306.5 Hz), 1.5 (4306.5 Hz), 1.6 (4341.8 Hz), 1.7 (4341.8 Hz), 1.8 (4376 Hz), 1.9 (4376 Hz), 1.12 (4746.2 Hz), 1.13

Figure 3.7 Modes for protofilament model.

(4748.2 Hz), 1.14 (4783.6 Hz), 1.15 (4786.2 Hz), 1.16 (4823.2 Hz), 1.17 (4825.8 Hz), 1.18 (4852 Hz), and 1.19 (4863.1 Hz).

This corresponds with a damping effect onto the cylinders from the resonator. In other words, the end cylinders oscillations have a destructive interference with the paired cylinders. Modes 1.1, 1.10, 1.11, and 1.20 can be said to have constructive interference.

Another point to highlight is the structure of the Protofilament Model shifting. The end cylinders do not remain unpaired. Instead, they pair (covalently bound) with the inner cylinders. This is unique to the Protofilament Model.

Spectrum for Su-Schrieffer-Heeger (SSH) and Protofilament Models. The spectrum shows Mode 1 has topological properties with the left portion being topologically trivial, the middle (0 mm) being the metal portion, and the right being topologically non-trivial. The Protofilament spectrum displays the same characteristics, indicating the Microtubule and Cancerous Models will exhibit topological properties within the lattice.
Eigenfrequency (Hz) vs. Parametric Sweep Value (mm)

a) Spectrum for SSH Model   b) Spectrum for Protofilament Model
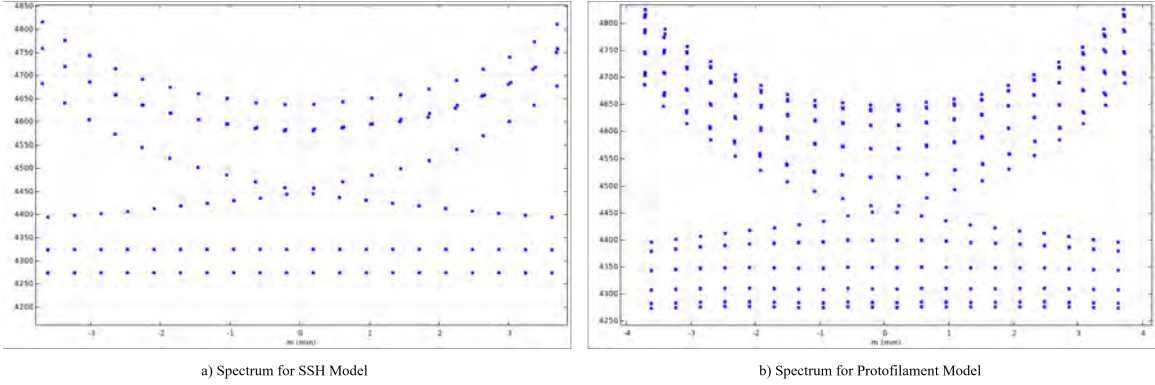
Figure 3.8 Spectrum for Su-Schrieffer-Heeger (SSH) and protofilament models.

Table 3.3 Frequencies for the First Mode of the Topological Study

Frequencies for Topological Study					
Frequencies for SSH Model		Frequencies for Protofilament Model			
Mode	Eigenfrequency (Hz)	Mode	Eigenfrequency (Hz)	Mode	Eigenfrequency (Hz)
1.1	4242.8	1.1	4272.8	1.11	4730.7
1.2	4322.9	1.2	4281.6	1.12	4746.2
1.3	4323.1	1.3	4281.7	1.13	4748.2
1.4	4390.4	1.4	4306.5	1.14	4783.6
1.5	4720.6	1.5	4306.5	1.15	4786.2
1.6	4789.8	1.6	4341.8	1.16	4823.2
1.7	4801.4	1.7	4341.8	1.17	4825.8
1.8	4853.4	1.8	4376	1.18	4852
–	–	1.9	4376	1.19	4853.8
–	–	1.10	4391.1	1.20	4863.1

CHAPTER 4

INVESTIGATING THE ENERGY HELD WITHIN A MICROTUBULE LATTICE

Chapter 4 will investigate the acoustic pressure held within the lattice of a healthy microtubule (Microtubule Model) and an unhealthy microtubule (Cancerous Model). Both structures took the information from the Protofilament Model to construct the two-dimensional lattice. However, the Cancerous Model has two distinct domains to simulate an unhealthy microtubule.

Various Views of the Microtubule Model. a) The xyz view that shows how energy translates through the lattice; b) The xy view; c) the yz view; and d) the xz view. The views and structures as the same for the Cancerous Model with the lattice coupling and end four cylinders having different coupling lengths.
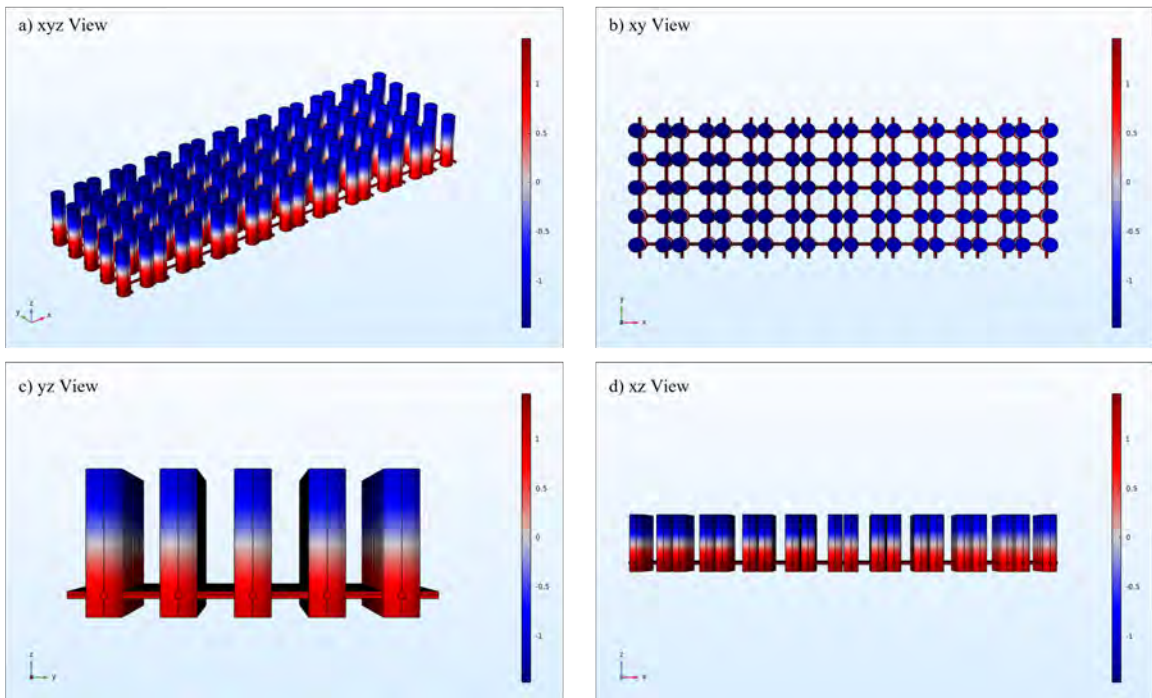
Figure 4.1 Various views of the microtubule model.

4.1 Microtubule Model

The Microtubule Model was composed of 5 rows of Protofilaments (20 cylinders, with 2 end cylinders and 9 pairs). End couplings were added to each side of the lattice, giving the structure end couplings on four sides. Typically, microtubules consist of 13 protofilaments, but the computational cost of 13 rowed lattice is too high. Therefore, the periodic conditions were extended to the four sides so the simulation could emulate a larger lattice without the high cost. Different views of the lattice are provided in Fig 4.1. The acoustic pressure plots agree with the Protofilament Model's plots. The eigenfrequencies are provided in Table 4.1.

Table 4.1 Frequencies for the Microtubule Model

| Mode	Eigenfrequency (Hz)	Mode	Eigenfrequency (Hz)	Mode	Eigenfrequency (Hz)	Mode	Eigenfrequency (Hz)	Mode	Eigenfrequency (Hz)
1.1	4239.4	1.21	4344.7	1.41	4439.5	1.61	4723.7	1.81	4845.4
1.2	4241.7	1.22	4346.1	1.42	4446	1.62	4728.3	1.82	4853.4
1.3	4248	1.23	4350.7	1.43	4450.4	1.63	4739.8	1.83	4859.1
1.4	4258.3	1.24	4354.6	1.44	4457	1.64	4748.5	1.84	4869
1.5	4259.4	1.25	4360.4	1.45	4469	1.65	4753.3	1.85	4875.6
1.6	4261.7	1.26	4362.4	1.46	4471.5	1.66	4761.1	1.86	4876.8
1.7	4268	1.27	4371.5	1.47	4485.1	1.67	4765.9	1.87	4880.5
1.8	4271.9	1.28	4375.4	1.48	4488.2	1.68	4767.9	1.88	4886.8
1.9	4278.4	1.29	4380.6	1.49	4496.7	1.69	4776.1	1.89	4891.6
1.10	4287.8	1.30	4381.3	1.50	4500.8	1.70	4783.7	1.90	4911.1
1.11	4292.1	1.31	4383	1.51	4507.8	1.71	4788.2	1.91	4915.7
1.12	4306.3	1.32	4389.5	1.52	4526.6	1.72	4789.6	1.92	4927.4
1.13	4308.2	1.33	4399.6	1.53	4543	1.73	4797.2	1.93	4932.5
1.14	4312.8	1.34	4400.3	1.54	4554.8	1.74	4800.6	1.94	4937.9
1.15	4315.2	1.35	4414.6	1.55	4558.9	1.75	4807.5	1.95	4945.7
1.16	4321.6	1.36	4415.5	1.56	4669.2	1.76	4812.1	1.96	4949.9
1.17	4324.1	1.37	4426.8	1.57	4680.3	1.77	4817.9	1.97	4973
1.18	4326.7	1.38	4430.8	1.58	4696.7	1.78	4822.7	1.98	4984.4
1.19	4332.2	1.39	4431.2	1.59	4703.7	1.79	4826.8	1.99	4995.1
1.20	4339.7	1.40	4437	1.60	4708.2	1.80	4833.2	1.100	5006.2

The spectrum for the Microtubule Model shows 4 distinguishable gaps. The one to note is the gap formed at $\approx$ 4700 Hz and $\approx$ 16 mm. The region spanning from 11 mm – 16 mm (Region 1) can be inferred to be where microtubule-associated

proteins (MAPs) are bound to the microtubule lattice. MAPs are bound to α-, β-tubulin dimers to help stabilize the microtubule. For example, the microtubule, which forms the mitotic spindle, needs to be stabilized during mitosis so the cell can divide properly. The region spanning from 16 mm – 20 mm (Region 2) is where the MAP is no longer bound. With the MAP no longer bound, the microtubule becomes unstable and can under dynamic instability, the continuous growing and shrinking of the microtubule.

Spectrum for Microtubule Model. There are four gaps, but the one of note is from 16 mm – 20 mm. Here it is believed that microtubule-assisted proteins (MAPs) unbind from α-,β-tubulin heterodimers at ≈ 4700 Hz.

Eigenfrequency (Hz) vs. Parametric Sweep Value (mm)

a) Full Spectrum for Microtubule Model   b) Expanded view of Microtubule Model
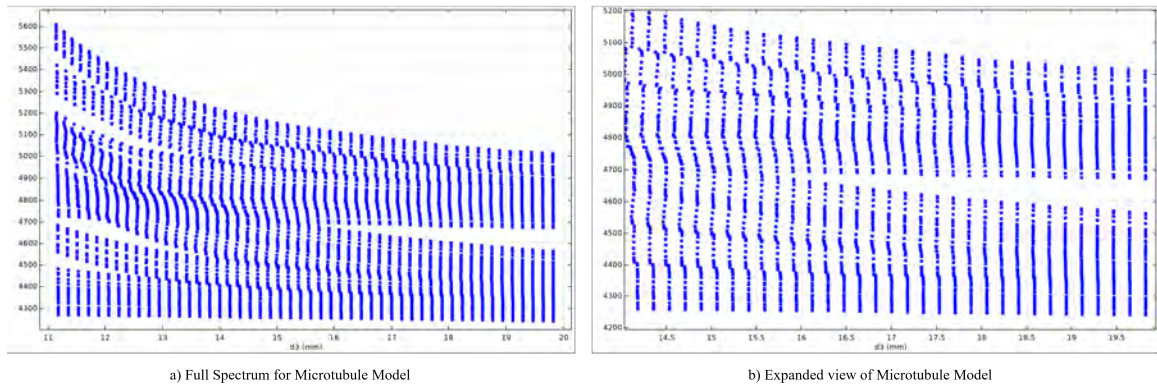
Figure 4.2 Spectrum for microtubule model.

4.2   Cancerous Model

The Cancerous Model was composed of 5 rows of Protofilaments (20 cylinders, with 2 end cylinders and 9 pairs), but the last four cylinders had different coupling strengths and the lattice coupling distance was increased. As stated in Chapter 2 Section 2.3, $d3 = 19$ mm (lattice coupling), $d4 = 14$ mm (weaker coupling), and $d5 = 20$ mm (stronger coupling). This was done to resemble a microtubule taken from a cancerous cell. They have been shown to have an 80 % - 20 % ratio of healthy/infected structure. Therefore, the first 16 cylinders from the Protofilament Model were taken, then the last four altered to weaken the interactions. The radius of coupling ($r2$)

Domains for Cancerous Model. To emulate the infected area of a cancerous microtubule, the end four cylinders coupling distances were changed to $d4 = 14$ mm (weaker) and $d5 = 20$ mm (stronger). Also, the lattice coupling, $d3$, was changed to 19 mm. These changes would generate different acoustic pressures.

a) Depiction of Cancerous Region of Microtubule   b) Cancerous Region of Microtubule within COMSOL Simulation
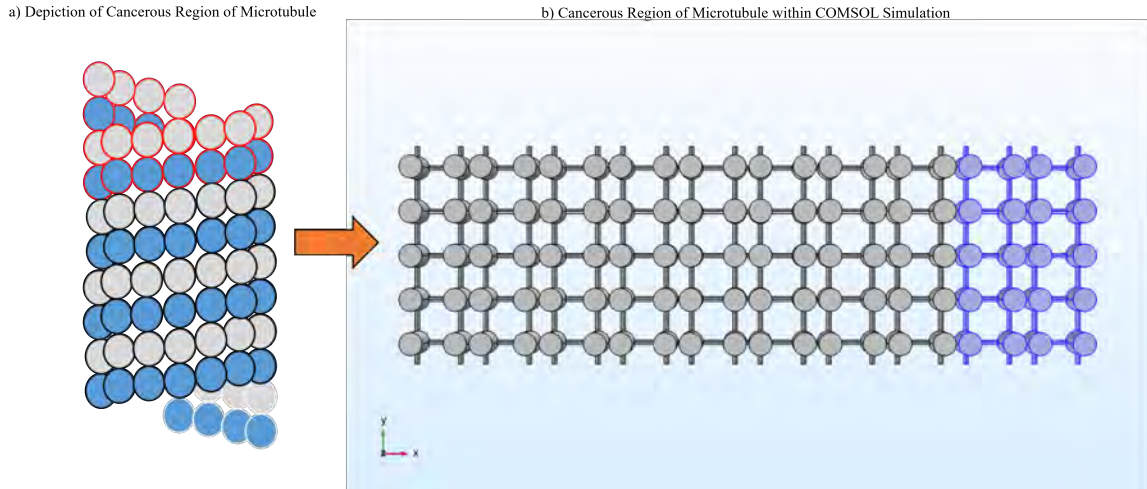
Figure 4.3 Domains for cancerous model.

could not be increased since the $r2$ had to be significantly smaller than the radius of the cylinder (r) for the spectrum to form.

The spectrum for the Cancerous Model agrees with the spectrum for the Microtubule Model indicating that MAPs are present in Region 1 but not in Region 2. This shows that the cell may still stabilize the microtubule even if unhealthy. However, there are differences in the acoustic pressure plots as indicated by Table 4.2 (Frequencies for the Cancerous Model). At Mode 1.56 (Microtubule – 4669.2 Hz; Cancerous – 4684.4 Hz), the eigenfrequencies increase. Indicating the resonator needs to put more driving force into the system to get oscillations. Fig 4.5 shows the acoustic pressure plot for both models at Mode 1.56.

Table 4.2 Frequencies for the Cancerous Model

Frequencies for Cancerous Study									
Mode	Eigenfrequency (Hz)	Mode	Eigenfrequency (Hz)	Mode	Eigenfrequency (Hz)	Mode	Eigenfrequency (Hz)	Mode	Eigenfrequency (Hz)
1.1	4239.3	1.21	4344.6	1.41	4439.3	1.61	4731.9	1.81	4852.3
1.2	4241.5	1.22	4346.2	1.42	4445.9	1.62	4737	1.82	4861.6
1.3	4247.9	1.23	4350.5	1.43	4450.2	1.63	4750.9	1.83	4867.4
1.4	4258.2	1.24	4354.5	1.44	4457	1.64	4756.7	1.84	4880
1.5	4259.3	1.25	4360.5	1.45	4468.8	1.65	4765.8	1.85	4881.7
1.6	4261.5	1.26	4362.8	1.46	4471.5	1.66	4770.8	1.86	4889.9
1.7	4268	1.27	4371.2	1.47	4485.1	1.67	4774.7	1.87	4890.9
1.8	4271.9	1.28	4375.2	1.48	4488.5	1.68	4777.3	1.88	4900.8
1.9	4278.3	1.29	4380.3	1.49	4496.3	1.69	4785.5	1.89	4903.7
1.10	4288.2	1.30	4381.3	1.50	4500.5	1.70	4793.3	1.90	4918.5
1.11	4292.1	1.31	4382.6	1.51	4507.7	1.71	4795.7	1.91	4920.8
1.12	4306.2	1.32	4389.3	1.52	4526.6	1.72	4799.8	1.92	4936.6
1.13	4308.7	1.33	4399.6	1.53	4543	1.73	4807.1	1.93	4940.2
1.14	4312.7	1.34	4400.1	1.54	4554.5	1.74	4811.3	1.94	4950.2
1.15	4315	1.35	4414.5	1.55	4558.7	1.75	4814.6	1.95	4958.3
1.16	4321.6	1.36	4415.5	1.56	4684.4	1.76	4822.6	1.96	4959.4
1.17	4324.1	1.37	4426.5	1.57	4695.4	1.77	4832.6	1.97	4978.6
1.18	4326.7	1.38	4430.6	1.58	4708.3	1.78	4832.9	1.98	4994.2
1.19	4332.2	1.39	4431.4	1.59	4712.1	1.79	4835.4	1.99	5008.7
1.20	4339.7	1.40	4436.9	1.60	4718.9	1.80	4845.6	1.100	5015.5

4.3   Region 2 Comparison

Since the spectrums for both the Microtubule and Cancerous Models are similar, a comparison of the acoustic pressure plots in Region 2 was completed. The gap in Region 2 opens at $\approx$ 4700 Hz. Therefore, to compare the acoustic pressure, the plots were taken at positions 14 mm, 16 mm, 18 mm, and 20 mm to see how pressure changes along the parametric sweep. The plots for 14 mm are virtually the same since this is still within Region 1.

The differences arise in Region 2 (16 mm – 20 mm). At 16 mm, the resonators have zero pressure for the Cancerous Model, while the Microtubule Model has zero pressure at the resonators and a small section inside. At 18 mm and 20 mm, the Cancerous Model has more zero pressure oscillators present (not vibrating with the lattice) than the Microtubule. This can be due to the rigidity within

Spectrum for Cancerous Model. There are four gaps, but the one of note is from 16 mm – 20 mm. The spectrum resembles the Cancerous Model spectrum indicating heterodimers stabilize even if unhealthy.

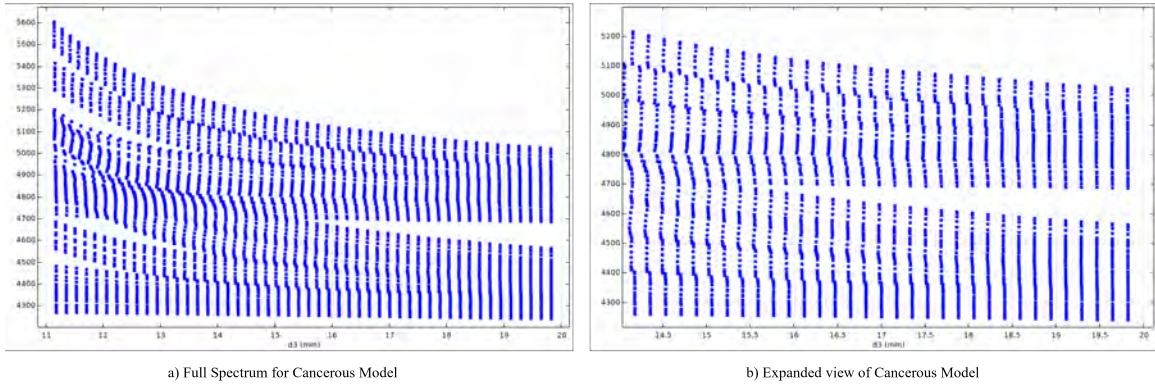Eigenfrequency (Hz) vs. Parametric Sweep Value (mm)

a) Full Spectrum for Cancerous Model

b) Expanded view of Cancerous Model

Figure 4.4 Spectrum for cancerous model.

Acoustic Pressure Comparison between Microtubule and Cancerous Models at Mode 1.56. a) The Microtubule Model at 1.56 (4669.2 Hz) and b) the Cancerous Model at 1.56 (4684.4 Hz). Mode 1.56 is where the frequencies begin to differentiate from each other, meaning the acoustic pressure plots behave differently. As seen, the energy held within the lattice (-3,3 for Microtubule and -2,2 for Cancerous) varies widely for Mode 1.56 and the remaining plots.

a) Microtubule Model at Mode 1.56 (4669.2 Hz)

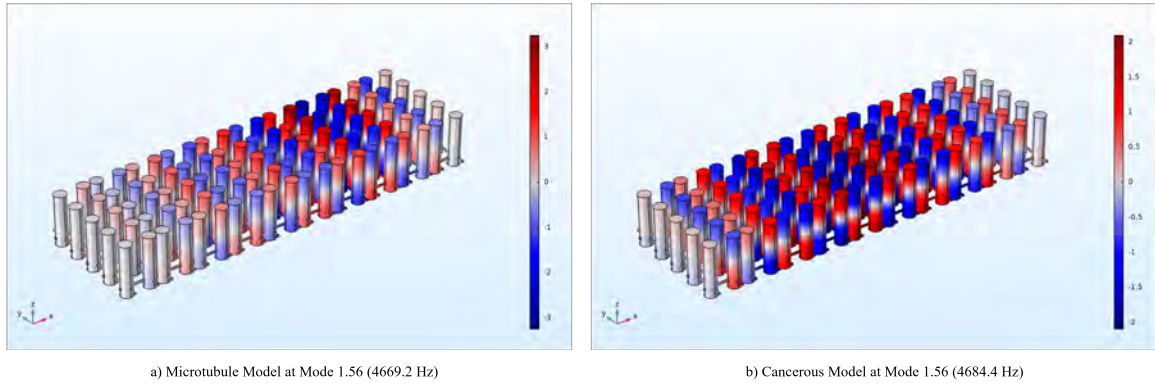b) Cancerous Model at Mode 1.56 (4684.4 Hz)

Figure 4.5 Comparison between microtubule and cancerous model at mode 1.56.

the Microtubule structure. Healthy microtubules are known to have rigidity than cancerous microtubules. The flexibility in the Cancerous Model can result in more 0 pressure oscillators, making the Cancerous Model hold less energy within its lattice.

Acoustic Pressure for Microtubule and Cancerous Models evaluated at ≈ 4700 Hz and 14 mm, 16 mm, 18 mm, & 20 mm. Pictures a) and e) were taken at 14 mm; pictures b) and f) were taken at 16 mm; pictures c) and g) were taken at 18 mm; and d) and h) were taken at 20 mm for the Microtubule and Cancerous Models, respectively. More zero pressure cylinders occur within the Cancerous Model as the parametric sweep goes approaches 20 mm indicating the Cancerous Model does not hold energy within the lattice as well as the Microtubule Model.
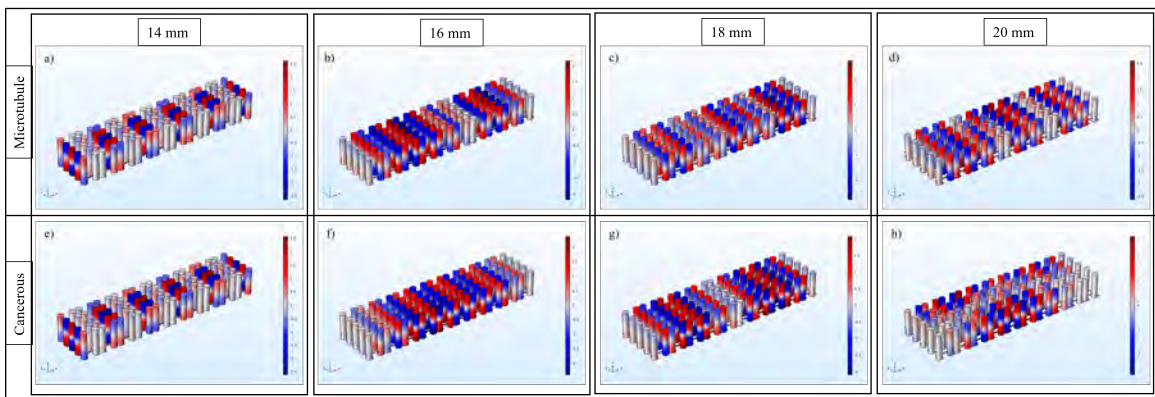

Figure 4.6   Acoustic pressure for microtubule and cancerous models evaluated at ≈ 4700 Hz and 14 mm, 16 mm, 18 mm, & 20 mm.

CHAPTER 5

DISCUSSION & CONCLUSION

The Microtubule and Cancerous Models proved to be effective models to simulate the lattice vibrations of a healthy and cancerous microtubule. The method to begin investigation is as follows: determine the best height and mode for study (Monomer, Dimer, and Trimer), examine the topology of the structure and expand it to fit known parameters of the microtubule (SSH and Protofilament), and create a lattice with periodic conditions to simulate the microtubule structure (Microtubule and Cancerous).

Spectrum Comparison between Microtubule and Cancerous Models. Both spectrums indicate that MAPs unbind from the lattice in Region 2. The gap forms within the same place, but the acoustic pressure varies within Region 2 as indicated in Figure 4.6. This indicates energy is held differently within the lattice of healthy and cancerous microtubules.
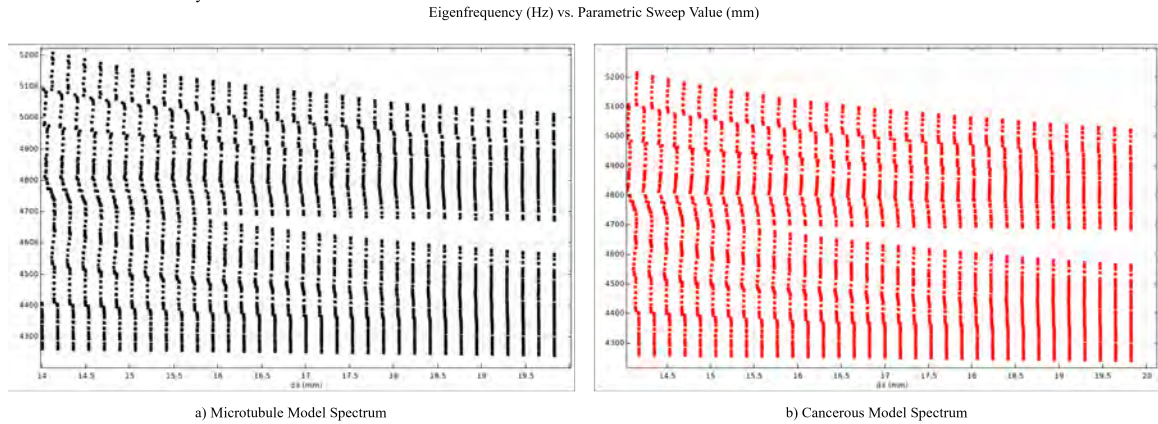
Eigenfrequency (Hz) vs. Parametric Sweep Value (mm)

a) Microtubule Model Spectrum   b) Cancerous Model Spectrum

Figure 5.1 Spectrum comparison between microtubule and cancerous models.

For this study, the best height was 40 mm and best mode was Mode 1. These two values gave the best separation between eigenfrequencies and little repetition. The SSH and Protofilament models indicates a significant bulk within the spectrum and topological solutions that are both trivial (left portion) and non-trivial (right portion), indicates there may be chiral symmetry. The Microtubule and Cancerous portions show MAPs present in Region 1 of the spectrum that stabilize the structure.

In Region 2, the MAPs unbind, and dynamic instability begins. There are more zero pressure points within the Cancerous Model, indicating it does not hold much energy within its lattice.

Proposed Schematics that will be used to alter the Microtubule and Cancerous Models in future works. a) The Microtubule and Cancerous Models will be altered to offset the upper portion of the lattice by shifting the upper region rightward as stated by Martinez et. al. b) The Microtubule and Cancerous Models will be altered to accommodate a larger resonator as stated by Deniz et. al.
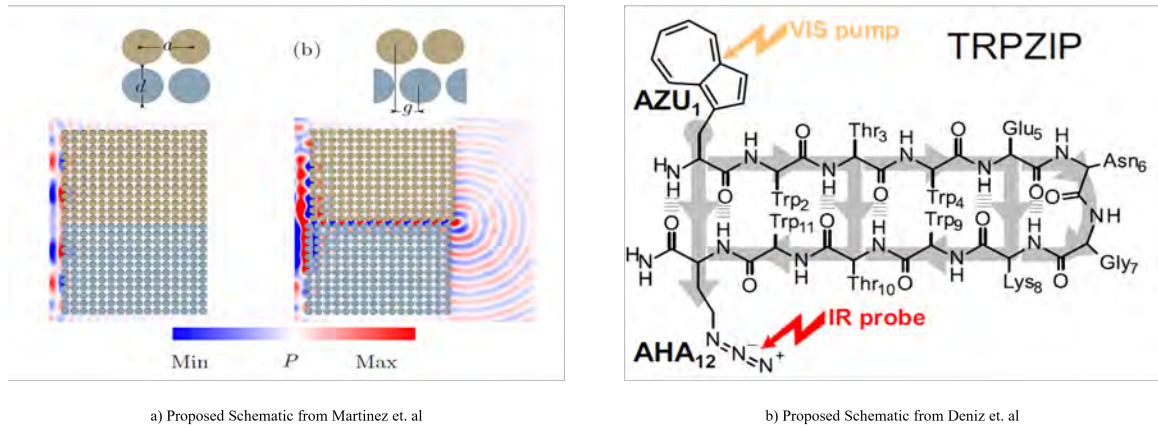

a) Proposed Schematic from Martinez et. al   b) Proposed Schematic from Deniz et. al

Figure 5.2 Proposed schematics that will be used to alter the microtubule and cancerous models in future works.

Future work involves altering the proposed structure to conform to the data presented by Martínez et al. [5] and Deniz et al. [4]. Martinez et al found the lattice structure is translated in the upper portion. Deniz et al found how vibrations flow topologically through the polyacetylene molecule, with the resonator being a larger molecule. Therefore, the proposed models will be altered to translate the upper portion of the lattice and to resonate the structure with a larger cylinder. In addition, cancerous microtubules will be grown and tracked to calculate the persistence length and experimental phononic spectrum (Aslam and Prodan [2]).

REFERENCES

[1] D.J. Apigo, W. Cheng, K.F. Dobiszewski, E. Prodan, and C. Prodan. Observation of topological edge modes in a quasiperiodic acoustic waveguide. *Phys. Rev. Lett.*, 122(9):095501, 2019. doi: 10.1103/PhysRevLett.122.095501.

[2] A.A. Aslam and C. Prodan. Experimentally measured phonon spectrum of microtubules. *J. Phys. D: Appl. Phys.*, 53(2):025401, 2019. doi: 10.1088/1361-6463/ab4bfb.

[3] W. Cheng, E. Prodan, and C. Prodan. Experimental demonstration of dynamic topological pumping across incommensurate bilayered acoustic metamaterials. *Phys. Rev. Lett.*, 125(22):224301, 2020. doi: 10.1103/PhysRevLett.125.224301.

[4] E. Deniz, L. Valiño-Borau, J.G. Löffler, K.B. Eberl, A. Gulzar, S. Wolf, P.M. Durkin, R. Kaml, N. Budisa, G. Stock, and J. Brendenbeck. Through bonds or contacts? mapping protein vibrational energy transfer using non-canonical amino acids. *Nature Communications*, 12(1):3284, 2021. doi: 10.1038/s41467-021-23591-1.

[5] J.A.I. Martínez, N. Laforge, M. Kadic, and V. Laude. Glide-reflection symmetric topological phononic crystal waveguide. URL https://arxiv.org/abs/2203.02692.

[6] E. Prodan and C. Prodan. Topological phonon modes and their role in dynamic instability of microtubules. *Phys. Rev. Lett.*, 103(24):248101, 2009. doi: 10.1103/PhysRevLett.103.248101.

[7] K. Qian, L. Zhu, K.H. Ahn, and C. Prodan. Observation of flat frequency bands at open edges and antiphase boundary seams in topological mechanical metamaterials. *Phys. Rev. Lett.*, 125(22):225501, 2020. doi: 10.1103/PhysRevLett.125.225501.